Frontiers in Scientific Research and Technology

Online ISSN: 2682-2970
Print ISSN: 2682-2962
http://fsrt.journals.ekb.eg

FSRT J 10 (2024) 18 – 30 10.21608/fsrt.2024.315451.1137

Geochemical investigations of the source rock intervals of the Oligocene Tineh Formation, offshore Nile Delta, Egypt

Nader A. A. Edress [1], Amr S. Deaf [2], Asmaa F. El-Moghazy [1,*]

[1]Geology Department, Faculty of Science, Helwan University, Ain Helwan, 11795 Cairo, Egypt

[2]Geology Department, Faculty of Science, Assiut University, Assiut, 71516, Egypt

ARTICLE INFO

Article history:
Received 25 August 2024
Received in revised form 24 September 2024
Accepted 28 September 2024
Available online 29 September 2024

Keywords
Gas-chromatography,
n-alkanes proxies,
Isoprenoids,
Biomarker

ABSTRACT

The gas chromatograms of the n-alkanes of the investigated Tineh Formation (Oligocene) show a dominance of short-chain n-alkanes with a slight admixture of medium-chain n-alkane components. They indicate the dominance of algae, microorganisms, Sphagnum moss and aquatic macrophytes. The low wax content (average 0.77), the low TAR value (0.01) and the high Paq value (average 0.91) show that submerged and floating seagrasses predominate over higher woody vascular plants in the studied formation. The redox potential based on the ratios of Pr/Ph (average 0.67) and Ph/n-C18 (average 0.32) of the Tineh samples indicates that an anoxic and dysoxic aquatic marine medium prevailed during the accumulation and preservation of OM. The low value of the ACL proxy (average 26.36) can also be attributed to the dominance of seagrass over woody plants, which took place in a relatively cool paleoclimate. The CPI shows an average value of about one (1.04), with two samples showing a value of less than one (samples C and D), which emphasizes the margin and the entry of the Tineh Formation into the main stage of maturation.

1. Introduction

The Neogene sediments of the offshore Nile Delta considered to have the greatest hydrocarbon potential for reservoir and source rocks (Shaaban et al., 2006; Zaghloul et al., 2001). Vandré et al. (2007) estimated from carbon isotope data that the offshore fields of the Nile Delta consist of mixed sources of biogenic and thermogenic origin. Dolson et al. (2001) and Hamdy et al. (2021) concluded that the base of the Neogene sediments in the offshore Nile Delta consists of thermogenic formations from Oligocene and Miocene.

Many sedimentological and stratigraphic studies have focused on the Oligocene sediments of the offshore Nile Delta (Cherif et al., 1993; El-Heiny I. and Enani H., 1996; Selim, 2018; Soliman and Orabi, 2000). In addition, Zakaria et al. (2019) carried out a high-resolution biostratigraphic sequence analysis for the Oligocene succession in the offshore Nile Delta. Later, El-Shafeiy et al. (2023) and El-Said et al. (2024) investigated the hydrocarbon potential and source properties of the Tineh Formation of Oligocene sediments. Farouk et al. (2023) and Farouk et al. (2024) use TOC, Rock-Eval pyrolysis and GC-MS procedures to evaluate organic geochemical features of the Upper Cretaceous–Pliocene sequence in the western offshore Nile Delta.

In the present study, a detailed geochemical gas chromatography analysis of the Oligocene Tineh Formation in the Habbar-1 well in the offshore Nile Delta (Fig. 1) is performed to evaluate the organic matter (OM) type, maturation stages and some of the paleoenvironmental depositional conditions such as redox potential and paleoclimate.

2. Geological setting

The Nile Delta is bounded by three major tectonic boundaries: the Red Sea Rift, the African-Anatolian and the Syrian Arc system (Ghassal et al., 2016). The tectonic evolution of the Nile Delta is controlled by three tectonic phases that extend from the Mesozoic (Middle Triassic) to present (Moustafa, 2020). Two phases are described as divergent tectonic movement and the third as convergent tectonic movement. Divergent tectonics is 1) Tethys rifting, which is responsible for the Neo-Tethys opening between the Afro-Arabian and Eurasian plates, 2) rifting, which causes the South Atlantic opening. On the other hand, convergent tectonism (Late Cretaceous to present) is responsible for the temporal change in the trend, which began with NW-SE faults and transitioned to a N–S fault trend in the Miocene (Moustafa, 2020; Tassy et al., 2015). The offshore areas of the Nile Delta show continued convergence and folding up to the present (Moustafa, 2020).

* Corresponding author at Helwan University

E-mail addresses: asmaa.fayek@science.helwan.edu.eg (Asmaa F. El-Moghazy)

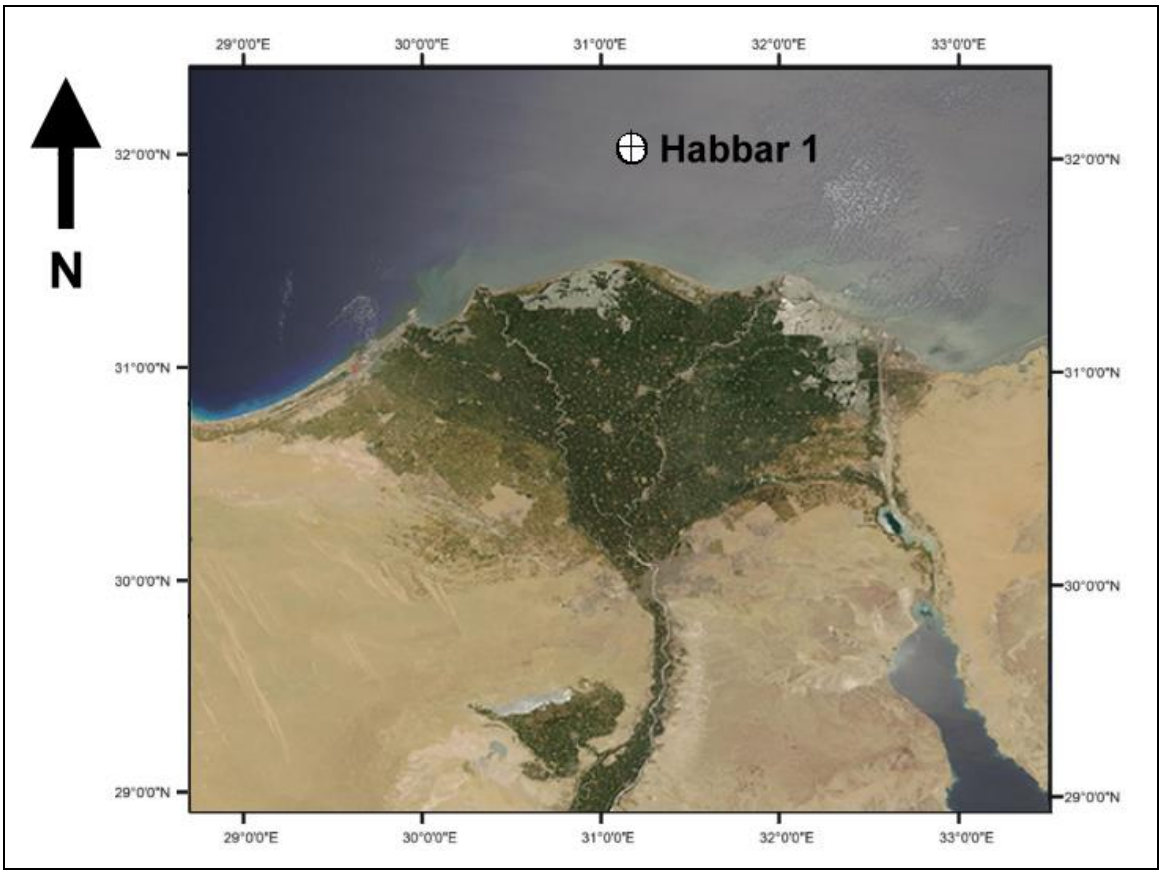

Fig. 1. Landsat image of the Nile Delta shows the location of studied Habbar-1 well, Nile Delta, Egypt.

During the early Oligocene, the African and Arabian plates diverged, causing dominant NW-trending faults that were responsible for the opening of the Gulf of Suez and the Red Sea (Bosworth, 1994; Patton et al., 1994). This in turn influenced the Nile Delta through eustatic sea-level fall (Guiraud and Bosworth, 1999; Selim, 2018).

Stratigraphically, the rock units of the Nile Delta range from Jurassic to Quaternary (Fig. 2). The rock units of the Neogene to Quaternary clastics are considered the most important for the hydrocarbon potential in the offshore Nile Delta (Nabawy and Shehata, 2015). The Oligocene sediments in the Nile Delta are represented by the Tineh Formation. This formation consists of marine to fluvio-marine shale and sandstone interbeds of middle Oligocene to late Miocene age (Fig. 2) (El-Heiny and Enani, 1996; El Heiny and Morsi, 1992). The Tineh Formation is unconformably underlain by the Appolonia Formation (middle Eocene) and unconformably overlain by the Qantara Formation (lower Miocene) (Fig. 2).

The Tineh Formation in the investigated Habbar-1 well consists mainly of greenish-grey shale with sandstone interbeds (Fig. 3). The sediments of the upper Oligocene to middle Miocene (Abu Zabal, Qantara and Sidi Salem formations) were not present in the studied Habbar-1 well in the offshore Nile Delta.

3. Material and methods

Eight ditch samples from depths of 4200 m to 4512 m were selected for GC analysis. The eight samples occupy only the middle part of the Tineh Formation, which extends from of 3852 m to 5130 m depth, with a vertical thickness of alternating argillaceous mudstone and sandstone, reaching 1371.5 m of Oligocene age in the studied Habbar-1 well. The samples are labeled alphabetically from A to H from top to bottom (Fig. 3). Samples were pulverized to 100 mesh and extracted with a Soxhlet apparatus for one day using a solvent of di-dichloromethane. After removal of the solvent by evaporation, the concentrated residue was analyzed using the GC instruments model (3400-GC) with a constant specification of 50 m Quadrex fused silica capillary column. The results obtained refer to the data analysis of the Nelson 3000 chromatography software. The calculation in the present study was based on the peak areas with integrated height in each chromatogram. GC analysis and identification of n-alkanes and isoprenoid peaks were performed at the Strato-Chem-Services, Cairo, Egypt.

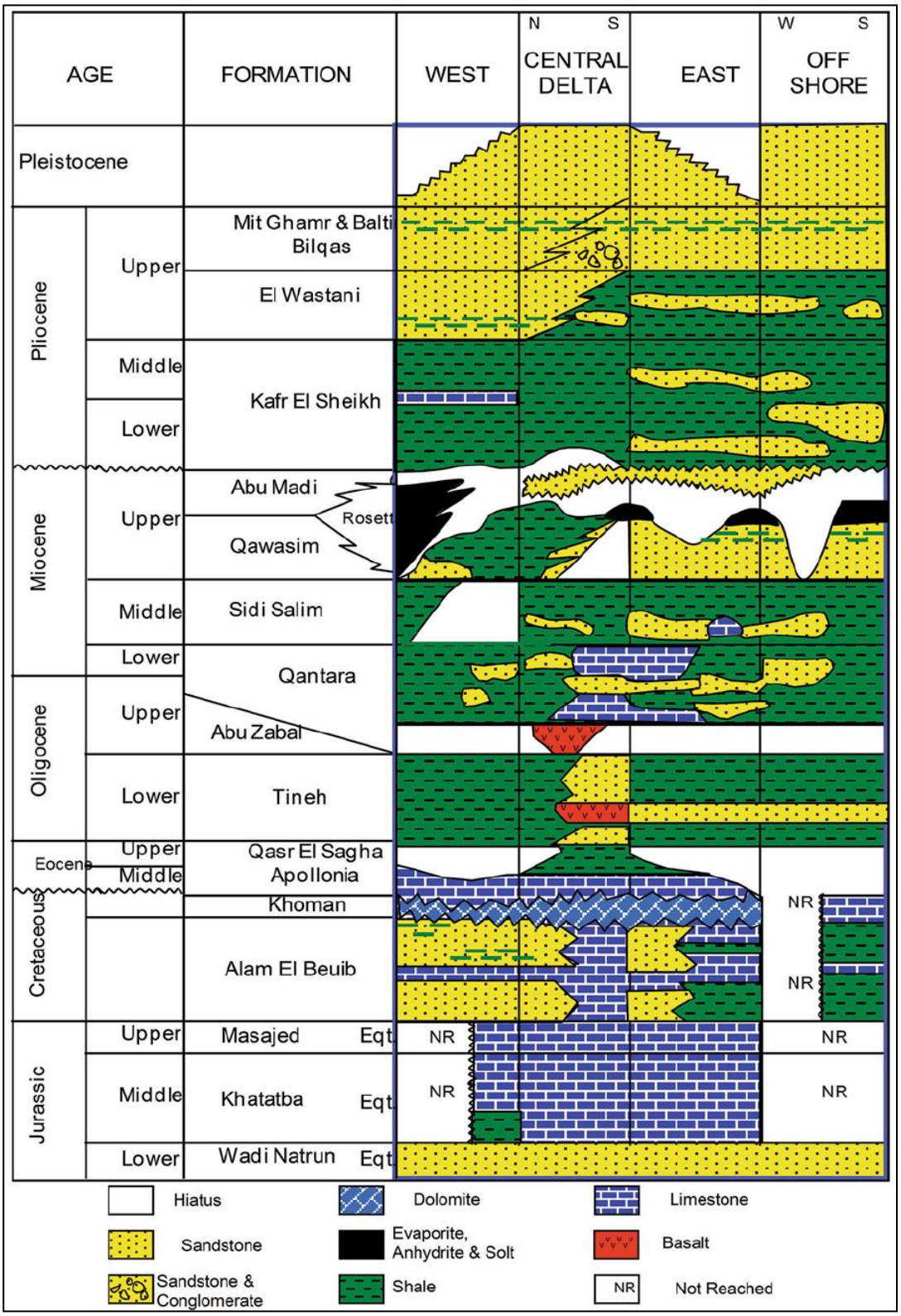

Fig. 2. Stratigraphic correlation chart for the Nile Delta region showing the Mesozoic−Cenozoic successions (EGPC, 1994; El-Said et al., 2024).

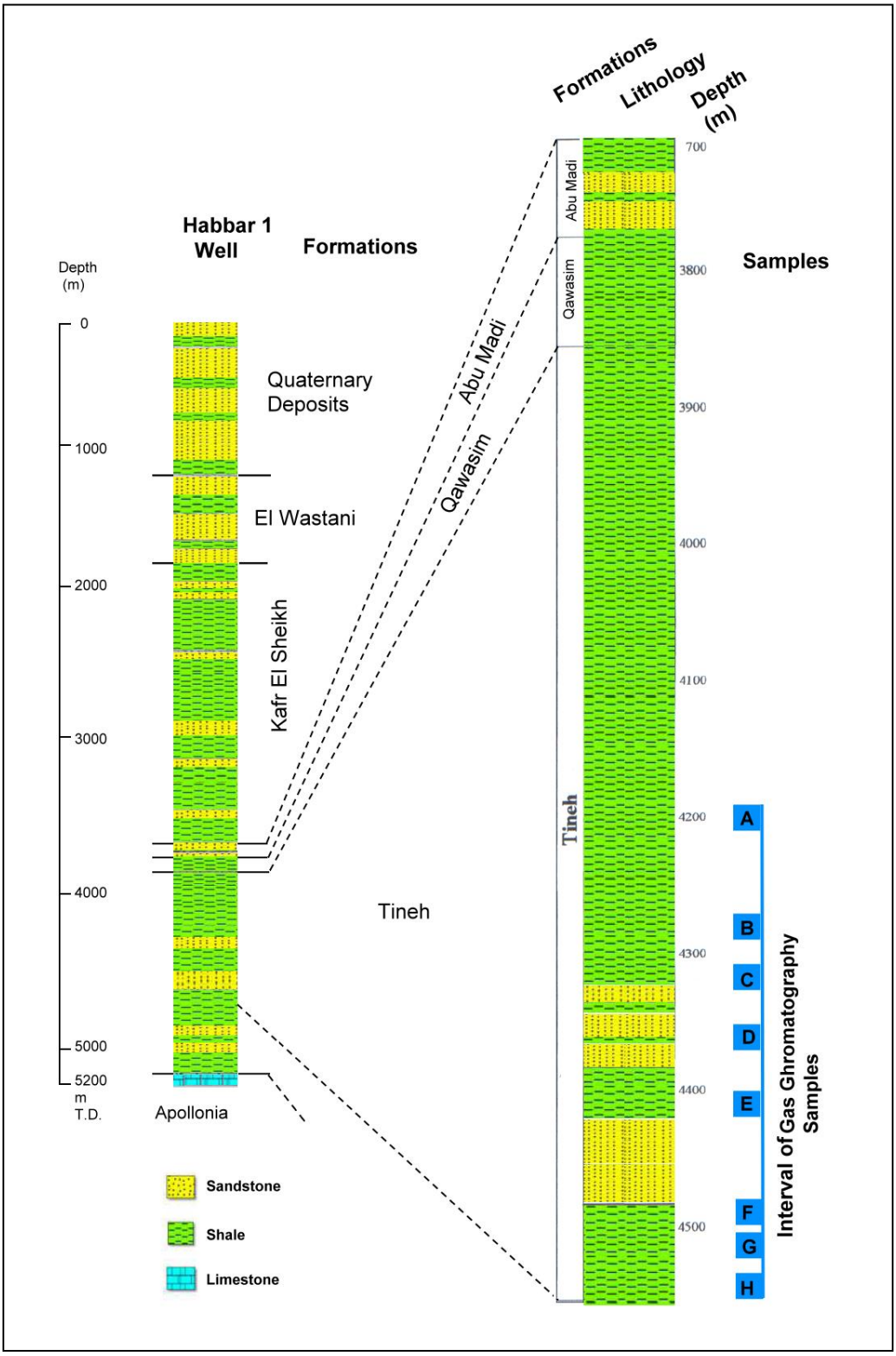

Fig. 3. The Lithostratigraphic column of Habbar-1 well with the studied GC samples (A – H) to the right of the column.

4. Results

The chromatograms of the eight samples analyzed show a distribution of the n-alkane peaks from n-C_{12} to n-C_{35} for all samples except for samples A and H, which start from n-C_{13} instead. All samples are characterized by a unimodal pattern with predominant maxima at an even peak of n-C_{18} (samples B, E and G), at an even peak of n-C_{20} (sample A) and an odd peak of n-C_{17} (sample F). The chromatograms also show maxima of two combined peaks of even and odd n-alkanes at n-C_{17} and n-C_{18} (samples C and D) and at n-C_{21} and n-C_{22} (sample H), as shown in Fig. 4. The isoprenoid of acyclic C_{19} (pristane) and C_{20} (phytane) are recorded in all studied samples (Fig. 4). The Pr/Ph ratio in the analyzed samples is between 0.42 and 0.87 with an average value of 0.67. The summarized results of the calculated and measured GC ratios and indices are shown in Table (1).

5. Discussion

5.1. OM precursor source based on n-alkanes Chain-length

The summation of ∑n-C_{15} to n-C_{20} is usually expressed as the precursor source of OM, which is mainly derived from photosynthetic microorganisms, algae and bacteria (Meyers, 2003). Chevalier et al. (2015) and Li et al. (2020) concluded that the main source of short-chain n-C_{15} and n-C_{17} is from algae, which are represented by chlorophyte and rhodophyte in the respective order. Zhao et al. (2022) also found that the short-chain n-alkanes generally originated from either microbial degradation and/or microbiological input. The Tineh samples of the present study show a maximum proportion of short-chain n-alkanes compared to mid- and long-chain n-alkanes and reach a maximum value of 55.06% (sample C) and a minimum value of 21.07% (sample B) with an average value of 42.22% (Table 1).

The mid-chain expressed by the summing ∑n-C_{21} to n-C_{25} primarily reflects the origin of the OM collection from both aquatic macrophytes and sphagnum moss (Chevalier et al., 2015; Zhao et al., 2022). Bingham et al. (2010) assumed that almost all Sphagnum moss species are characterized by the dominance of odd n-alkanes (n-C_{23}). Ficken et al. (2000) and Mead et al. (2005) concluded that mainly the odd-numbered mid-chains (n-C_{21}, n-C_{23} and n-C_{25}) are due to the deposition conditions of the macrophytes in aquatic environments either in fresh-water and/or coastal marine-water. The percentages of mid-chains in the present samples of the Tineh Formation are the next in abundance and vary between values of 51.72% (sample H) and 16.44% (sample B) with an average value of 32.47%. The present result realized that the OM of the studied formation contains a considerable amount of aquatic macrophytes mainly in the form of seagrass.

In contrast to the previous short- and mid-chain ones, Ficken et al. (2000) found that the long-chain ∑n-C_{27}-n-C_{31} of n-alkanes were accumulated and preserved in terrestrial vascular higher plants. Mead et al. (2005) and Liu et al. (2022) suggested that the odd -chain n-alkanes ≥ n-C_{27} (n-C_{27}, n-C_{29}, n-C_{31}) are an indicator of the predominance of terrestrial plants. The long-chain percentages of the Tineh Formations are expressed by a low percentage value (2.28%-9.23%; average 4.58%), reflecting a low percentage contribution of a terrigenous plant.

The very long-chain summation ∑≥n-C_{33} is indicative of the higher plants deposited in a warm paleoclimate when they are present in a considerably high amount (El Nemr et al., 2016; Jeng, 2006). However, in the present study of the Tineh samples, they have a tiny percentage close to zero of a very-long-chain (0.04-0.13%; average 0.1%), which can be attributed to a cold and temperate paleoclimate instead of warmer paleoclimate.

By plotting the percentages of the short-, mid- and long-chain fractions of the Tineh samples in the ternary diagram of Zhao et al. (2022) (Fig. 5). Almost all samples are in the range of algae and microorganisms, two samples are in the range of sphagnum mosses and aquatic macrophytes. The latter two samples belong to the upper and lower part of the investigated Lower Tineh Formation of samples A and H (Table 1; Fig. 5).

In general, the OM of the lower Tineh Formation consists of microorganisms and algae with a considerable amount of aquatic macrophytes, which increase in the uppermost and lowermost parts of the investigated formations (samples A and H) (Table 1). The low percentage of long-chain and very long-chain n-alkanes in the analyzed samples (≈5%) could indicate depositional conditions from terrestrial land plant sources far from open seawater.

5.2. Biomarker indices and proxies

5.2.1. The natural n-alkanes ratio (NAR)

The NAR is a ratio determined by Mille et al. (2007) to estimate the proportion of petroleum and natural n-alkanes sources. The ratio is close to 1 for intact plants that are either more terrestrial or marine. In contrast, in the case of petroleum and petroleum-derived hydrocarbons, the NAR approaches zero or even minus (El Nemr et al., 2016; Kanzari et al., 2014; Yazis et al., 2016). In other words, the NAR distinguishes the OM of intact plant tissues from those undergoing diagenesis, catagenesis or even metagenesis stage of maturation. The calculated NAR for the studied Tineh Formation shows a minus (-0.6; sample B) and low values of (0.1; samples C, D, F and G) with an average value equal to zero. The NAR of zero value realizes the OM are the petroleum hydrocarbon sources, and the Tineh Formation may enter to a stage or subsequent stages of maturated levels.

5.2.2. The waxiness degree

Peters et al. (2005) determine the wax content to distinguish the OM of marine sources, which is characterized by a low wax content <1 from the OM of the terrigenous sources which is characterized by a high molecular weight of waxiness contents >1. El Diasty and Moldowan (2013) suggested OM with a wax content more than one is generally referred to as a terrestrial organic source. The wax content of the studied samples shows a low wax content between 0.25 and 0.71 (average 0.77) (samples B to G).

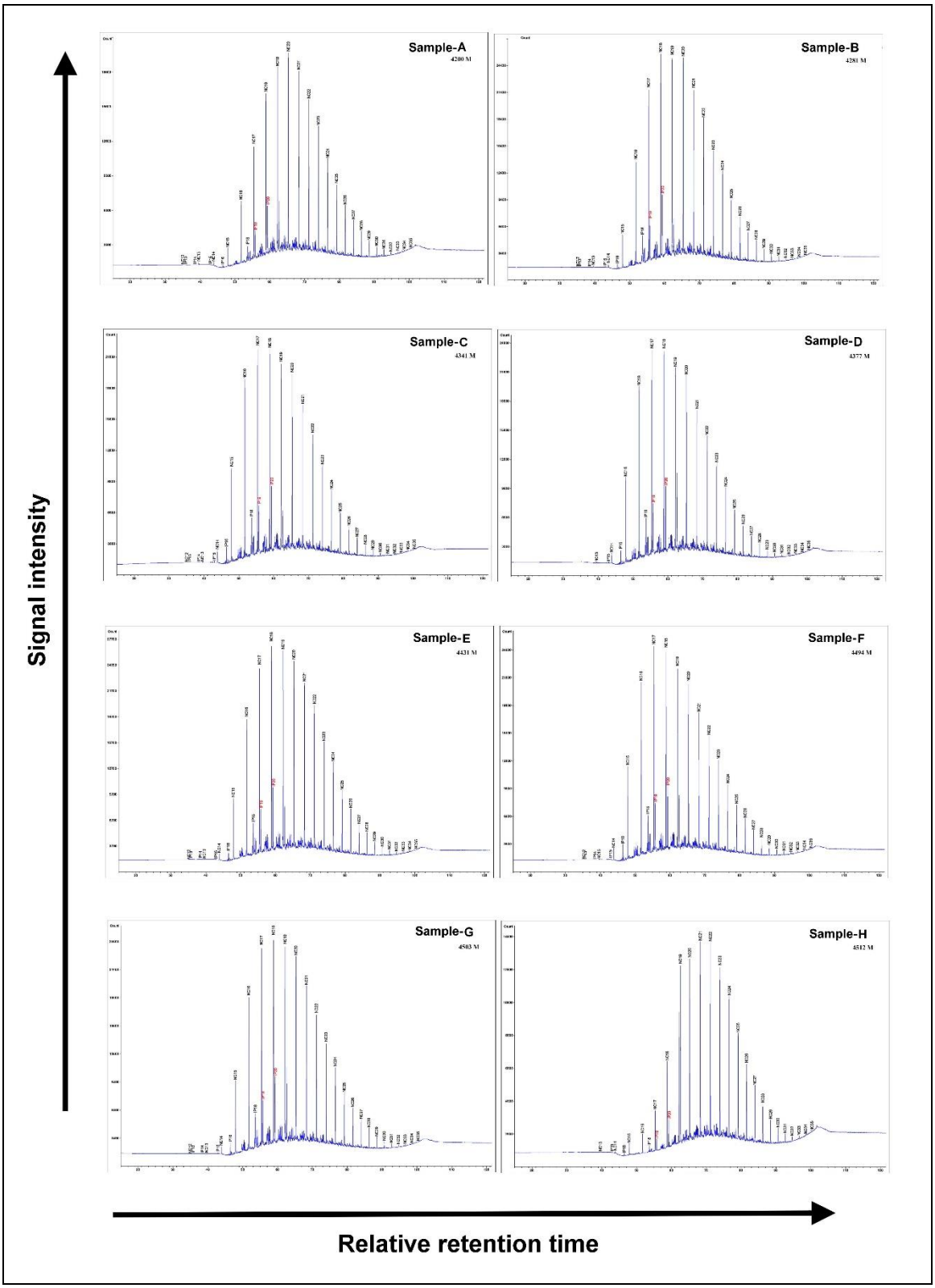

Fig. 4. Normal (NC) and isoprenoids (IP) alkanes chromatograms of eight samples of the lower Tineh formation.

Table. 1. The summarized calculation of the GC proxy and indices using the integrated height area of the Chromatograms of the eight extracted samples belongs to the Lower Tineh formation (Late Oligocene), Habar-1 well, offshore Nile-Delta.

Sample no.	Depth (m)	(%) ∑n-C_{15-19} Short-chain	(%) ∑n-C_{21-25} Mid-chain	(%) ∑n-C_{27}-n-C_{31} Long-chain	(%) ≥ n-C_{33} Very long-chain	NAR	Degree of waxiness	CPI	n-C_{27}/n-C_{17}	TAR	Paq	ACL_{25-33}	Pr/Ph	Pr/n-C_{17}	Ph/n-C_{18}
A	4200	35.50	40.76	6.30	0.13	0.07	1.04	1	0.32	0.01	0.89	26.49	0.57	0.25	0.31
B	4281	21.07	16.44	2.28	0.04	-0.60	0.25	1.09	0.17	0.00	0.90	26.39	0.66	0.24	0.31
C	4341	55.06	28.36	2.55	0.08	0.10	0.49	0.97	0.09	0.00	0.94	26.12	0.74	0.24	0.33
D	4377	53.71	29.03	3.20	0.11	0.10	0.53	0.93	0.10	0.01	0.93	26.24	0.78	0.25	0.33
E	4431	47.05	33.64	4.77	0.09	0.08	0.71	1.10	0.16	0.01	0.90	26.41	0.70	0.24	0.31
F	4494	53.70	28.68	3.94	0.08	0.10	0.54	1.08	0.12	0.01	0.91	26.39	0.77	0.24	0.32
G	4503	50.19	31.14	4.34	0.06	0.10	0.62	1.11	0.14	0.01	0.91	26.42	0.70	0.23	0.32
H	4512	21.49	51.72	9.23	0.22	0.10	2.00	1.07	1.39	0.02	0.89	26.44	0.42	0.29	0.32
Average		**42.22**	**32.47**	**4.58**	**0.10**	**0**	**0.77**	**1.04**	**0.31**	**0.01**	**0.91**	**26.36**	**0.67**	**0.25**	**0.32**

CPI (carbon preference index) = ((n-C_{25}+n-C_{-27}+n-C_{29}+n-C_{31}+n-C_{33})/(n-C_{24}+n-C_{26}+n-C_{28}+n-C_{30}+n-C_{32})/(n-C_{25}+n-C_{27}+n-C_{29}+n-C31+n-C_{31})/(n-C_{26}+n-C_{28}+n-C_{30}+n-C_{32}+n-C_{34}))/2; NAR (natural n-alkanes ratio) = (∑n-C_{19-33})-(2*∑n-C_{20-32}/∑n-C_{19-33});; Degree of Waxiness = (∑n-C_{21-31})/∑n-C_{15-20}); ACL_{25-33} (proxy ratio) = (25*n-C_{25}+27*n-C_{27}+29*n-C_{29}+31*n-C_{31}+33*n-C_{33}/(n-C_{25}+n-C_{27}+n-C_{29}+n-C_{31}+n-C_{33}); Paq (aquatic non-emergent macrophytes/ aquatic emergent and terrestrial macrophytes ratio) = (n-C_{23}+n-C_{25})/(n-C_{23}+n-C_{25}+n-C_{29}+n-C_{31}); TAR (terrigenous / aquatic ratio) = (n-C_{27}+n-C_{29}+n-C_{31})/(n-C_{15}+n-C_{17}+n-C_{19}).

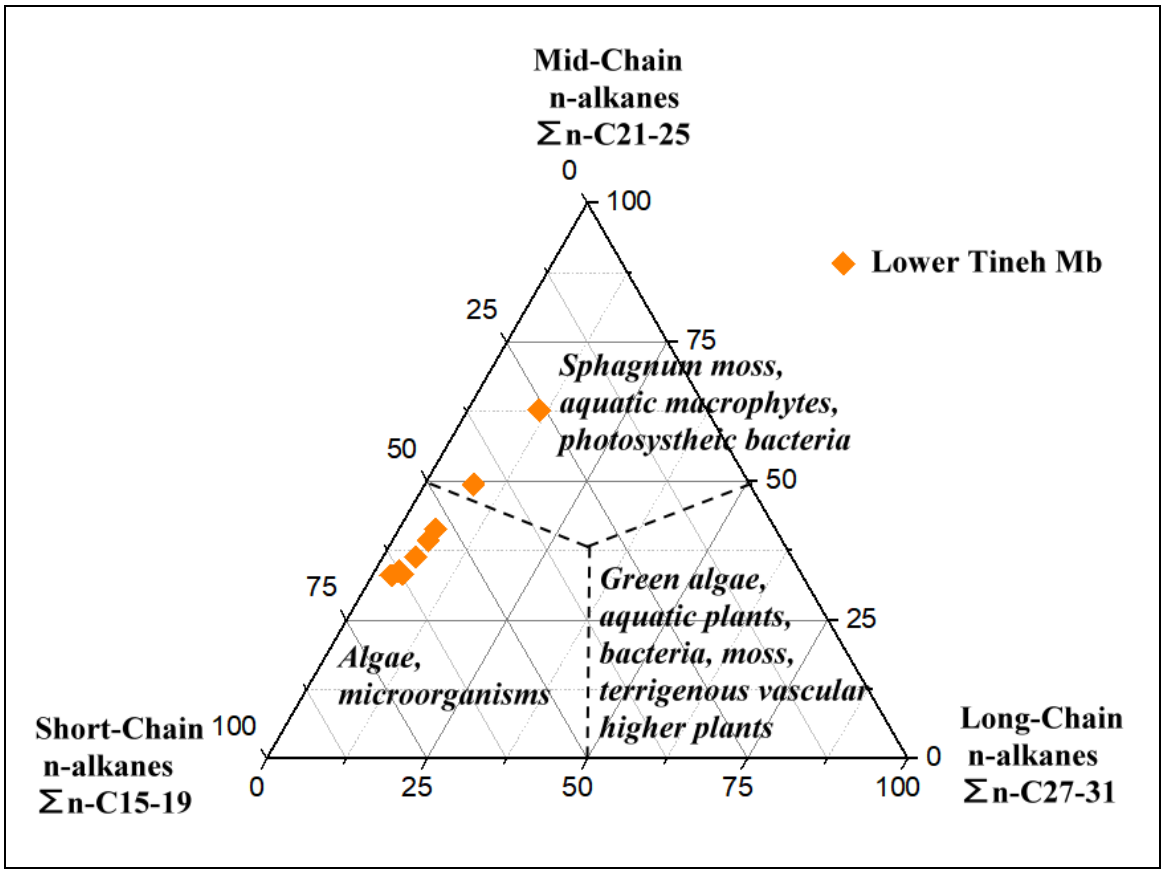

Fig. 5. Cross-plot of the lower Tineh samples on ternary of a short-, mid-, and long-chain diagram (after Zhao et al., 2022).

These low wax samples represent 222 m of the lower Tineh Formation from a depth 4282 m to 4503 m.

While the uppermost and lowermost samples of A and H of the same Tineh Formation have a degree of wax >1 (1.04 and 2 respectively), which characterizes the terrestrial plant input in these parts of the studied formation.

Plotting the studied samples on the Pr/Ph ratio against the El Diasty and Moldowan (2013) proxy diagram of the waxiness degree showed that almost all studied samples are located in a range of marine OM sources characterized by reduction environments, except for two samples of A and H, which are located in OM sources of terrestrial origin characterized by oxidation environments (Fig. 6).

5.2.3. The carbon performance index (CPI)

The CPI is a proxy first used by Bray and Evans (1961) to represent the dominance of odd over even n-alkanes in the ranges between n-C_{25} and n-C_{33} (Hunt, 1995). The CPI has two indices: one indicative of maturity (if CPI > 1, the source rock is immature, and if it is < 1, the source rock is mature) and the second indicative of OM origin (if the CPI is between 5-10 high, it is indicative of higher plant OM source; and if it is relatively low, it is indicative of OM derived from bacteria, algae and microorganisms) (Commendatore et al., 2012; Filho et al., 2021; Kanzari et al., 2014, 2012).

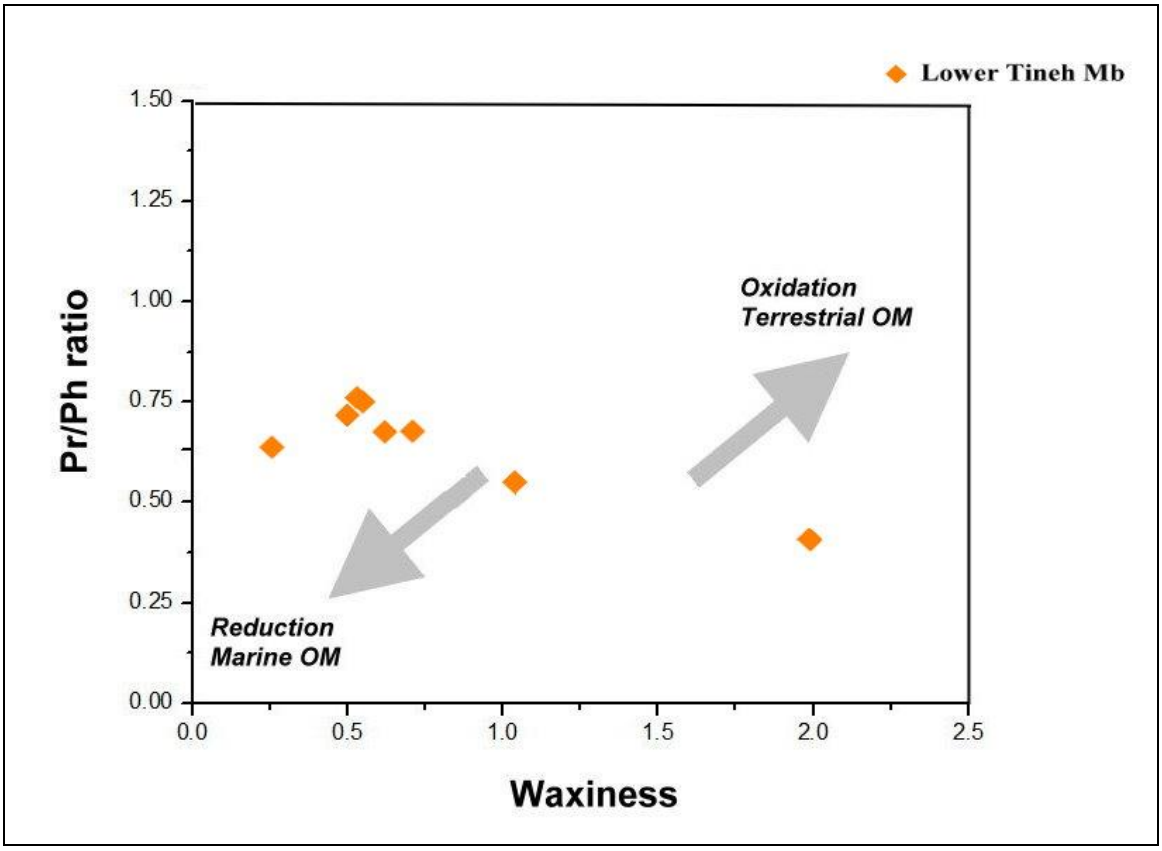

Fig. 6. Cross plot of the lower Tineh samples on the Pr/Ph versus a degree of waxiness Diagram (after El Diasty and Moldowan, 2013).

In the present study, the CPI of the Tineh samples has an average value of 1, with two samples (C and D) having a CPI value less than 1, indicating that the Tineh Formation has already entered the main stage of maturation (oil window). The lower CPI values of the studied samples also indicate the dominance of bacteria, algae and microorganisms over terrestrial land plants as the main component of the OM.

Plotting the eight samples analyzed on the CPI against the Pr/Ph ratio according to the diagram by Meyers and Snowdon (1993), all samples lie in the left part of the diagram and belong to the marine and hyper-saline carbonate and/or evaporite sources (Fig. 7).

5.2.4. The n-C_{27}/n-C_{17} ratio

The n-C_{27}/n-C_{17} ratio is a ratio established by Katz and Lin (2014) to differentiate the source of OM belonging to either the lacustrine or marine depositional environments. They found that OM of lacustrine origin generally has a high n-C_{27}/n-C_{17} ratio of more than 1 and can reach a value of 2, while OM of marine origin generally has a low value of less than 1. The measured n-C_{27}/n-C_{17} values of the Tineh samples show very low values in the range of 0.14 and 0.3 (average 0.31), except for sample H, which has a value of

1.39 (Table 1). Based on the above results, the lowest part of the Tineh (sample H) shows a lacustrine origin, while all the youngest samples above it shows a marine origin. The latter could indicate marine transgression events from sample H upwards to sample G until A.

5.2.5. The Terrigenous/aquatic ratio (TAR)

The TAR suggested quantification of in situ terrestrial versus algal OM by determining the concentration of long-chain versus short-chain n-alkanes according to Bourbonniere and Meyers (1996). The high TAR ratio of values above 25 was an indication of the dominance of terrigenous over aquatic input (Filho et al., 2021; Mille et al., 2007).

The studied samples show very low values of the TAR ratio, ranging from 0 to 0.02 (average 0.01), indicating that the OM components of microorganisms and algae predominate over the terrigenous OM components.

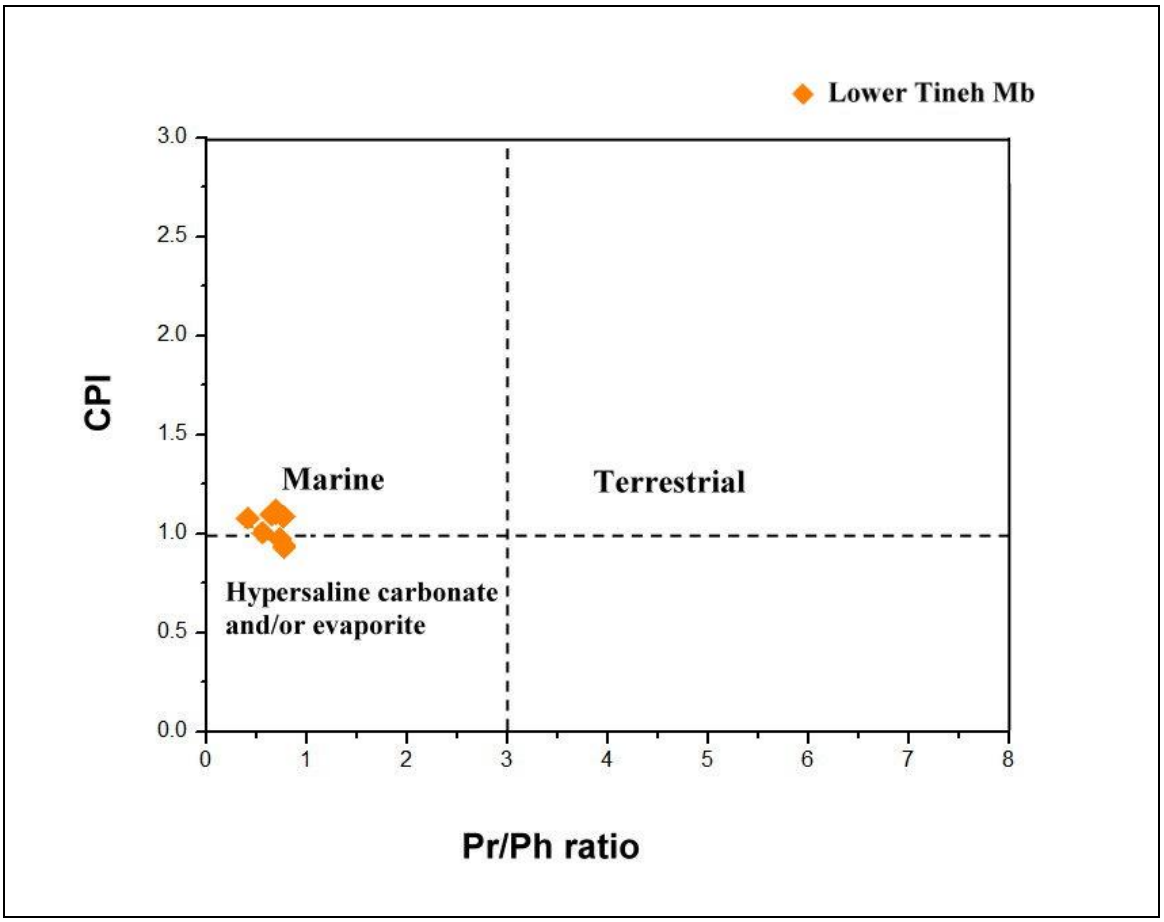

Fig. 7. Cross-plat of the lower Tineh samples on the CPI against Pr/Ph ratio diagram (Meyers and Snowdon, 1993).

5.2.6. The proxy of aquatic macrophytes (Paq)

The Paq proxy is used to quantify the different plant types (Cranwell et al., 1987). Meyers (2003) used Paq as a ratio between aquatic non-emergent macrophytes and aquatic emergent and terrestrial macrophytes. Moreover, (Li et al., 2020) identified three different categories of macrophytes based on the amounts of the Paq proxy. These categories are terrestrial higher plant TE (Paq = <0.2-0.24), submerged and floating plant SF (Paq = 0.64-≥0.86) and emergent plants EM (Paq = 0.16-0.4). The high Paq values in the studied samples refer to the second category SF and not to the first category TE and the third category EM.

The relatively highest Paq values of the Tineh samples with a range between 0.89 and 0.94 (average 0.91) coincide with the high value of the SF categories for submerged and floating plant. The Paq values may also relate to the increased proportion of aquatic non-emergent plants in the seawater medium according to Meyers (2003).

5.2.7. The average chain length proxy (ACL)

The ACL proxy is a paleoclimate indicator (Gagosian and Peltzer, 1986). In warmer climate region, the plant biosynthesize process produced a long chain OM with high melting point coating wax, whereas plants in cooler regions were characterized by a short-chain OM and lower wax content (Poynter and Eglinton, 1990). In addition, Wei et al. (2015) supposed that the ACL value depends on the dominance of grass plant over woody plants. ACL decreases when grass plant increase and increases when woody plants increase.

Li et al. (2020) recently related ACL values to vegetation temperature and assumed that ACL>30 mainly corresponds to an increase in temperature and ACL<29 to a decrease in temperature. The calculated ACL values in the samples of the present study show relatively low values mainly below 29 within a narrow range of 26.12 and 26.29 (average 26.36), which is related to both cooler and warmer paleoclimate and/or the dominance of grasses over woody plants in the OM-containing precursor environments.

5.2.8. The Pr/Ph, Pr/n-C_{17} and Ph/n-C_{18} ratios

The Pr/Ph ratio is generally used as a redox potential ratio for the depositional environment in which OM accumulates and is preserved (Hunt, 1995). The dysoxic-suboxic environment is characterized by a Pr/Ph ratio greater than 1, while the anoxic state is mainly characterized by Pr/Ph ratio less than 1 (Zhao et al., 2020). The Pr/Ph of the studied Tineh samples shows a low Pr/Ph ratio in the range of 0.42 and 0.78 (average 0.67), indicating the dominance of the anoxic condition during the preservation of OM in the Tineh Formation.

Moreover, the Tineh samples were plotted in the redox potential diagram of Pr/Ph versus Ph/n-C_{18} according to Wu et al. (2023) (Fig. 8). All the samples are located in the dysoxic environment. The dysoxic transition zone is characterised by a low oxygen content <30 in an aqueous medium (Edress et al., 2023).

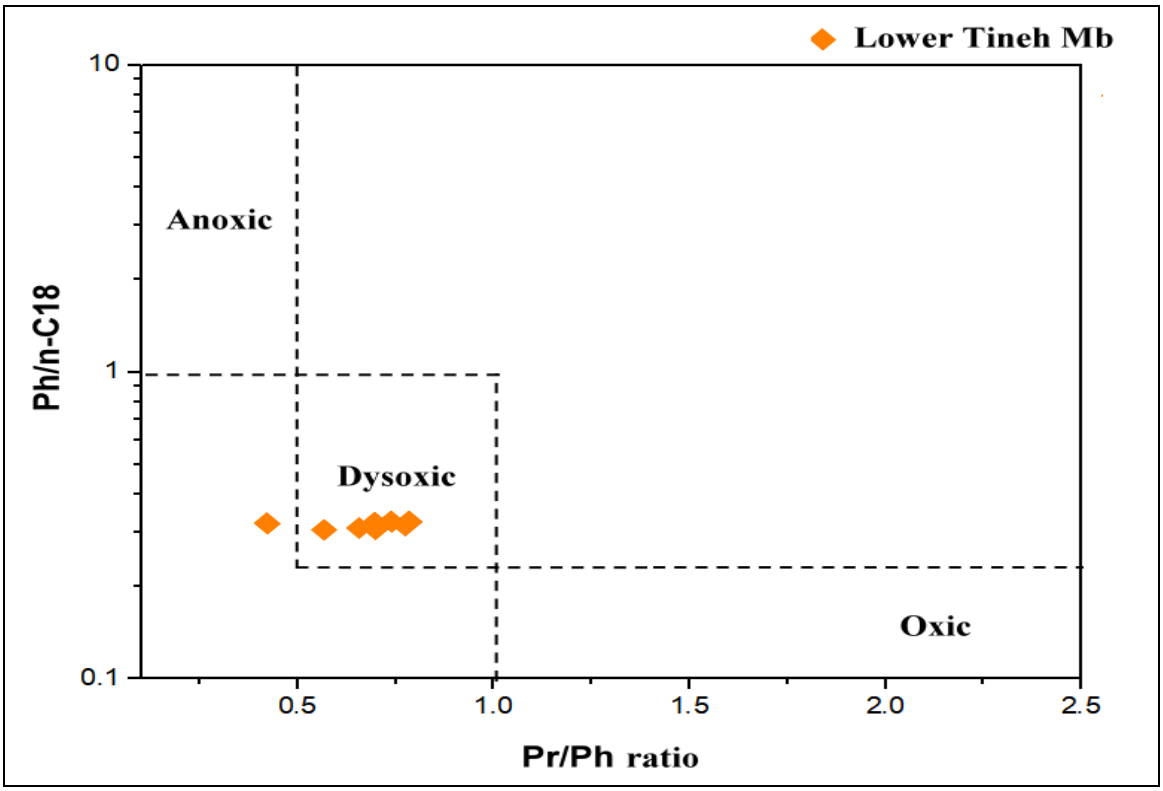

Fig. 8. Cross-plot of the studied lower Tineh formation on the Pr/Ph versus Ph/n-C_{18} redox potential diagram (Wu et al., 2023).

Mathur et al. (1988) used the Pr/n-C_{17} ratio as an indicator of the depositional environment, either from an aquatic marsh with a Pr/n-C_{17} ratio >1 or from open seawater with Pr/n-C_{17} <0.5. The studied Tineh samples have a Pr/n-C_{17} ratio of 0.24 to 0.29 (average 0.25), confirming that deposition occurred in open seawater.

When the studied Tineh samples are plotted on the Pr/Ph ratio against the Pr/n-C_{17} ratio of Connan and Cassou (1980), all the samples lie within the quadratic range of marine origin OM (Fig. 9).

The ratio of Ph/n-C_{18} to Pr/n-C_{17} was used by Shanmugam (1985) to explain the depositional environment and types of kerogens (Fig. 10). Plotting the investigated samples on the diagram of Shanmugam (1985), the studied samples in the lower corner of the diagram of mature OM belong to marine OM environments, with a few transitional samples, and are mainly composed of type II and II/III kerogens with strong reducing conditions (Fig. 10).

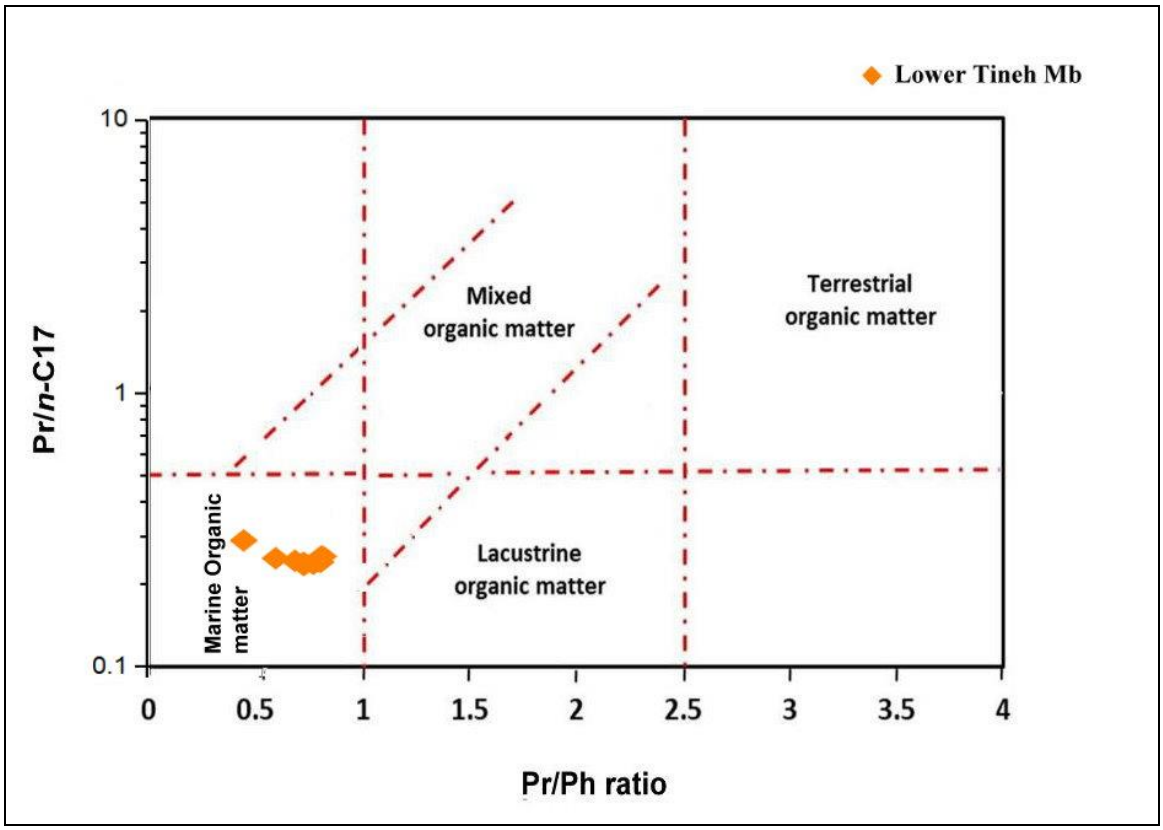

Fig. 9. Cross-Plot of the studied lower Tineh samples on the Pr/Ph versus Pr/n-C17 diagram (Connan and Cassou, 1980).

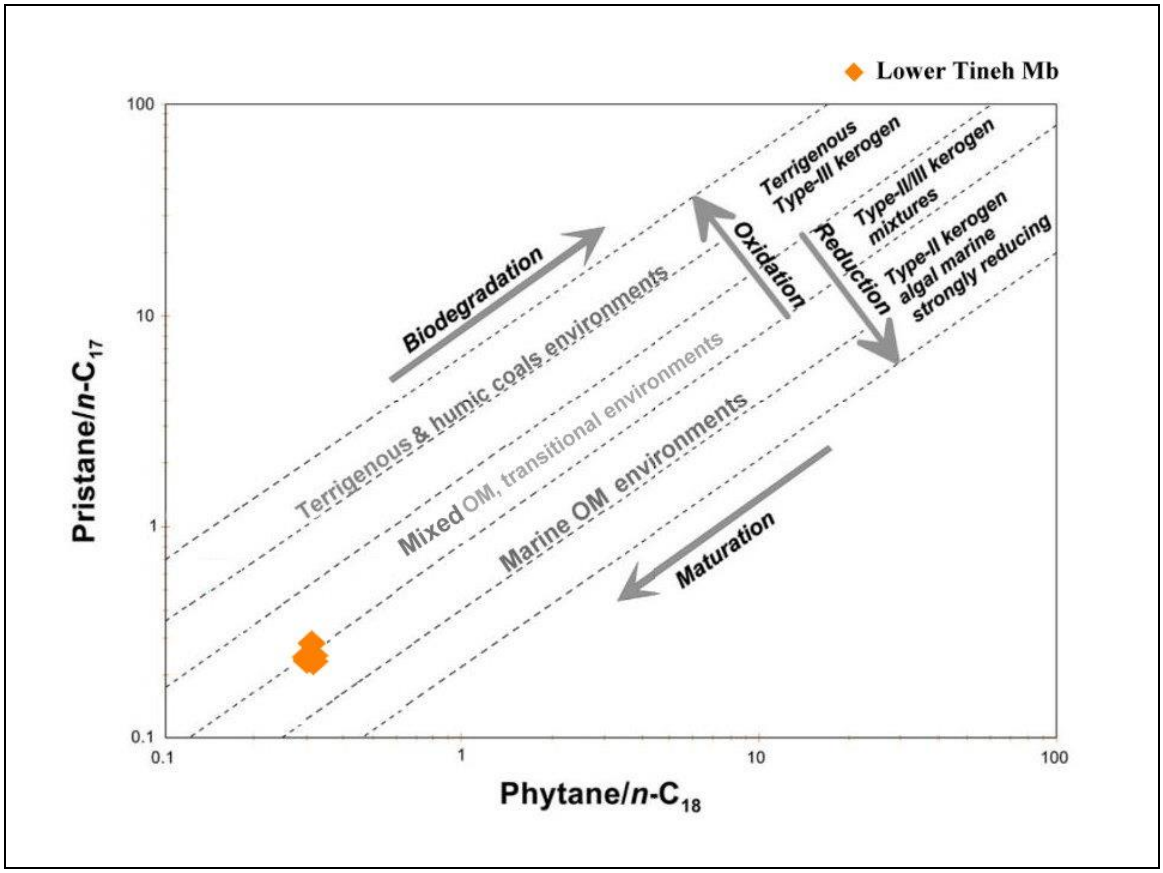

Fig. 10. Cross-Plot of the Lower Tineh samples on the Pr/n-C_{17} versus Ph/n-C_{18} diagram (Shanmugam, 1985).

Conclusion

The short-chain and mid-chain n-alkanes are the major constituent of the OM-containing lower Tineh Formation with proportions of 42.22% and 32.47% in the respective order. The present study shows that algae and microorganisms are the main components of OM bearing Tineh Formation, which mainly consists of algae and aquatic macrophytes of type II and type II/III kerogens. The high value of the Paq proxy provides additional insight into the composition of the OM supporting the Tineh Formation of submergent and floating seagrasses. The redox potential reveals the dominance of dysoxic and anoxic conditions, based on the ratios Pr/Ph <1 and Ph/n-C_{18} (average 0.32). CPI and NAR suggest that the Tineh Formation is entering the marginal maturity stage of hydrocarbon sources. A low ACL proxy (average 26.36) indicates the dominance of cooler paleoclimate over the warmer one. The n-C_{27}/n-C_{17} ratio confirms the deposition of the entire Tineh Formation in marine environments except for the lowermost part (sample H) in shallower lacustrine environments.

References

Bingham, E.M., McClymont, E.L., Väliranta, M., Mauquoy, D., Roberts, Z., Chambers, F.M., Pancost, R.D., Evershed, R.P., 2010. Conservative composition of n-alkane biomarkers in Sphagnum species: implications for palaeoclimate reconstruction in ombrotrophic peat bogs. Org. Geochem. 41, 214–220.

Bosworth, W., 1994. A model for the three-dimensional evolution of continental rift basins, north-east Africa. Geol. Rundschau 83, 671–688.

Bourbonniere, R.A., Meyers, P.A., 1996. Sedimentary geolipid records of historical changes in the watersheds and productivities of Lakes Ontario and Erie. Limnol. Oceanogr. 41, 352–359.

Bray, E.E., Evans, E.D., 1961. Distribution of n-paraffins as a clue to recognition of source beds. Geochim. Cosmochim. Acta 22, 2–15.

Cherif, O.H., El-Sheikh, H., Mohamed, S., 1993. Planktonic foraminifera and chronostratigraphy of the Oligo-Miocene in some wells in the isthmus of Suez and the North-Eastern reach of the Nile Delta, Egypt. J. African Earth Sci. (and Middle East) 16, 499–511.

Chevalier, N., Savoye, N., Dubois, S., Lama, M.L., David, V., Lecroart, P., Le Ménach, K., Budzinski, H., 2015. Precise indices based on n-alkane distribution for quantifying sources of sedimentary organic matter in coastal systems. Org. Geochem. 88, 69–77. https://doi.org/https://doi.org/10.1016/j.orggeochem.2015.07.006

Commendatore, M.G., Nievas, M.L., Amin, O., Esteves, J.L., 2012. Sources and distribution of aliphatic and polyaromatic hydrocarbons in coastal sediments from the Ushuaia Bay (Tierra del Fuego, Patagonia, Argentina). Mar. Environ. Res. 74, 20–31.

Connan, J., Cassou, A.M., 1980. Properties of gases and petroleum liquids derived from terrestrial kerogen at various maturation levels. Geochim. Cosmochim. Acta 44, 1–23. https://doi.org/https://doi.org/10.1016/0016-7037(80)90173-8

Cranwell, P.A., Eglinton, G., Robinson, N., 1987. Lipids of aquatic organisms as potential contributors to lacustrine sediments—II. Org. Geochem. 11, 513–527.

Dolson, J.C., Shann, M. V, Matbouly, S., Harwood, C., Rashed, R., Hammouda, H., 2001. The petroleum potential of Egypt, In: Downey, M.W., Threet, J.C., Morgan, W. A. (Eds.), Petroleum Provinces of the Twenty-First Century, AAPG Memoir 74.

Edress, N.A.A., Abdel-Rahman, E.A., Abdel-Wahab, M.G.F., 2023. Geochemical significance for the composition and depositional environments of the Campanian carbonate-rich phosphorite, Abu-Tartur plateau, Western Desert, Egypt. J. African Earth Sci. 202, 104938.

EGPC, 1994. Nile Delta & North Sinai fields, Discoveries and Hydrocarbon Potentials: A Comprehensive Overview. Egypt. Gen. Pet. Cairo, Egypt 387.

El-Heiny I., Enani H., 1996. Regional stratigraphic interpretation pattern of Neogene sediments, Northern Nile Delta, in: Belayim Petroleum Company, 13th. Exploration and Production Conference, EGPC, Cairo. pp. 270–290.

El-Said, M.M., Abd-Allah, A.M.A., Abdel-Aal, M.H., Hakimi, M.H., Lashin, A.A., Abd-El-Naby, A., 2024. Geochemistry of Liquid Hydrocarbons and Natural Gases Combined with 1D Basin Modeling of the Oligocene Shale Source Rock System in the Offshore Nile Delta, Egypt. ACS Omega 9, 11780–11805. https://doi.org/10.1021/acsomega.3c09245

El-Shafeiy, M., Abdel Halim, N., El-Kammar, M., El-Bakry, G., 2023. Oligocene source-rock characteristics and hydrocarbon generation modeling of the eastern Nile delta, Egypt. Geoenergy Sci. Eng. 227. https://doi.org/10.1016/j.geoen.2023.211884

El Diasty, W.S., Moldowan, J.M., 2013. The Western Desert versus Nile Delta: A comparative molecular biomarker study. Mar. Pet. Geol. 46, 319–334.

El Heiny, I., Morsi, S., 1992. Stratigraphic correlation of the Neogene sediments in the eastern Nile Delta and Gulf of Suez, Egypt, E.G.P.C., in: 11th Exploration and Production Conference, V1,. pp. 166–192.

El Nemr, A., Moneer, A.A., Ragab, S., El Sikaily, A., 2016. Distribution and sources of n-alkanes and polycyclic aromatic hydrocarbons in shellfish of the Egyptian Red Sea coast. Egypt. J. Aquat. Res. 42, 121–131.

Farouk, S., Khairy, A., Shehata, A.M., Uguna, C.N., El Sheennawy, T., Salama, A., Al-Kahtany, K., Meredith, W., 2023. Geochemical evaluation and hydrocarbon generation potential of the Upper Cretaceous–Pliocene succession, offshore Nile Delta, Egypt. J. African Earth Sci. 205, 105004. https://doi.org/10.1016/j.jafrearsci.2023.105004

Farouk, S., Sen, S., Ahmad, F., Al-Kahtany, K., Benmamar, S., Abdeldaim, A., 2024. Assessment of pore pressure in the Oligocene–Pleistocene stratigraphy of the West Delta Deep Marine, offshore Nile Delta, Egypt. Mar. Geophys. Res. 45. https://doi.org/10.1007/s11001-023-09536-x

Ficken, K.J., Li, B., Swain, D.L., Eglinton, G., 2000. An n-alkane proxy for the sedimentary input of submerged/floating freshwater aquatic macrophytes. Org. Geochem. 31, 745–749. https://doi.org/doi:10.1016/s0146-6380(00)00081-4

Filho, S., J, P., Andrade, G.O., Moreira, K., Rockenbach, C.K., 2021. Determination of aliphatic hydrocarbons in surface sediments of Mangueira Lagoon (RS—Brazil). Environ. Earth Sci. 80, 1–11.

Gagosian, R.B., Peltzer, E.T., 1986. The importance of atmospheric input of terrestrial organic material to deep sea sediments. Org. Geochem. 10, 661–669.

Ghassal, B.I., El Atfy, H., Sachse, V., Littke, R., 2016. Source rock potential of the Middle Jurassic to middle Pliocene, onshore Nile Delta basin, Egypt. Arab. J. Geosci. 9, 1–21.

Guiraud, R., Bosworth, W., 1999. Phanerozoic geodynamic evolution of northeastern Africa and the northwestern Arabian

platform. Tectonophysics 315, 73–104.

Hamdy, D., El-Bakry, G., El Habaak, G.H., El-Shafeiy, M., 2021. Characteristics and generation modeling of some source rocks in the South Eastern offshore Mediterranean area, Egypt. Mar. Pet. Geol. 123, 104719.

Hunt, J.M., 1995. Petroleum geochemistry and geology (textbook). Pet. Geochemistry Geol. (Textbook).(2 nd Ed.), WH Free. Company, 743.

Jeng, W.-L., 2006. Higher plant n-alkane average chain length as an indicator of petrogenic hydrocarbon contamination in marine sediments. Mar. Chem. 102, 242–251.

Kanzari, F., Syakti, A.D., Asia, L., Malleret, L., Mille, G., Jamoussi, B., Abderrabba, M., Doumenq, P., 2012. Aliphatic hydrocarbons, polycyclic aromatic hydrocarbons, polychlorinated biphenyls, organochlorine, and organophosphorous pesticides in surface sediments from the Arc river and the Berre lagoon, France. Environ. Sci. Pollut. Res. 19, 559–576.

Kanzari, F., Syakti, A.D., Asia, L., Malleret, L., Piram, A., Mille, G., Doumenq, P., 2014. Distributions and sources of persistent organic pollutants (aliphatic hydrocarbons, PAHs, PCBs and pesticides) in surface sediments of an industrialized urban river (Huveaune), France. Sci. Total Environ. 478, 141–151.

Katz, B., Lin, F., 2014. Lacustrine basin unconventional resource plays: Key differences. Mar. Pet. Geol. 56, 255–265.

Li, C., Ma, S., Xia, Y., He, X., Gao, W., Zhang, G., 2020. Assessment of the relationship between ACL/CPI values of long chain n-alkanes and climate for the application of paleoclimate over the Tibetan Plateau. Quat. Int. 544, 76–87.

Liu, J., Zhao, J., He, D., Huang, X., Jiang, C., Yan, H., Lin, G., An, Z., 2022. Effects of plant types on terrestrial leaf wax long-chain n-alkane biomarkers: Implications and paleoapplications. Earth-Science Rev. 235, 104248.

Mathur, S., Jain, V.K., Tripathi, G.K., Jassal, J.K., Chandra, K., 1988. Biological marker geochemistry of crude oils of Cambay Basin, India. Pet. Geochemistry Explor. Afro-Asian Reg. Balkema, Rotterdam 459, 473.

Mead, R., Xu, Y., Chong, J., Jaffé, R., 2005. Sediment and soil organic matter source assessment as revealed by the molecular distribution and carbon isotopic composition of n-alkanes. Org. Geochem. 36, 363–370.

Meyers, P.A., 2003. Applications of organic geochemistry to paleolimnological reconstructions: a summary of examples from the Laurentian Great Lakes. Org. Geochem. 34, 261–289.

Meyers, P.A., Snowdon, L.R., 1993. Types and Thermal Maturity of Organic Matter Accumulated During Early Cretaceous Subsidence of the Exmouth Plateau, Northwest Australian Margin: Chapter 8 119–130. https://doi.org/https://doi.org/10.1306/St37575C8

Mille, G., Asia, L., Guiliano, M., Malleret, L., Doumenq, P., 2007. Hydrocarbons in coastal sediments from the Mediterranean Sea (Gulf of Fos area, France). Mar. Pollut. Bull. 54, 566–575.

Moustafa, A.R., 2020. Mesozoic-Cenozoic Deformation History of Egypt. Springer International Publishing. https://doi.org/10.1007/978-3-030-15265-9_7

Nabawy, B., Shehata, A., 2015. Integrated petrophysical and geological characterization for the Sidi Salem-Wakar sandstones, offshore Nile Delta. Egypt J Afr Earth Sci 110:, 160–175.

Patton, T.L., Moustafa, A.R., Nelson, R.A., Abdine, S.A., 1994. Tectonic evolution and structural setting of the Suez rift: chapter 1: Part I. Type basin: Gulf of Suez.

Peters, K.E., Walters, C.C., Moldowan, J.M., 2005. The Biomarker Guide, Second Edition, Volume II, in: Biomarkers and Isotopes in Petroleum Systems and Earth History, United Kingdom at the Cambridge University Press,. p. 684 P.

Poynter, J., Eglinton, G., 1990. 14. Molecular composition of three sediments from hole 717c: The Bengal fan, in: Proceedings of the Ocean Drilling Program: Scientific Results. pp. 155–161.

Selim, S.S., 2018. Sedimentological architecture, shelf-edge trajectories and evolution of an Oligocene reservoir, East Nile Delta. Geol. Mag. 155, 747–771.

Shaaban, F., Lutz, R., Littke, R., Bueker, C., Odisho, K., 2006. Source-rock evaluation and basin modeling in NE Egypt (NE Nile Delta and northern Sinai). J. Pet. Geol. 29, 103–124.

Shanmugam, G., 1985. Significance of coniferous rain forests and related organic matter in generating commercial quantities of oil, Gippsland Basin, Australia1. Am. Assoc. Pet. Geol. Bull. 69, 1241–1254.

Soliman, I.S., Orabi, H.. O., 2000. Oligocene stratigraphy and paleoecology of two 630 Mediterranean offshore wells, in North Sinai, Egypt. Al-Azhar Bull. Sci. 11, no. 63, 187–201.

Tassy, A., Crouzy, E., Gorini, C., Rubino, J.-L., Bouroullec, J.-L., Sapin, F., 2015. Egyptian Tethyan margin in the Mesozoic: Evolution of a mixed carbonate-siliciclastic shelf edge (from Western Desert to Sinai). Mar. Pet. Geol. 68, 565–581.

Vandré, C., Cramer, B., Gerling, P., Winsemann, J., 2007. Natural gas formation in the western Nile delta (Eastern Mediterranean): Thermogenic versus microbial. Org. Geochem. 38, 523–539.

Wei, Z., Wang, Y., Wu, B., Wang, Z., Wang, G., 2015. Paleovegetation inferred from the carbon isotope composition of long-chain n-alkanes in lacustrine sediments from the Song-nen Plain, northeast China. J. Paleolimnol. 54, 345–358.

Wu, P., Dujie, H., Cao, L., Zheng, R., Wei, X., Ma, X., Zhao, Z., Chen, J., 2023. Paleoenvironment and Organic Characterization of the Lower Cretaceous Lacustrine Source Rocks in the Erlian Basin: The Influence of Hydrothermal and Volcanic Activity on the Source Rock Quality. ACS omega 8, 1885–1911.

Yazis, M., Asia, L., Piram, A., Doumenq, P., Syakti, A.D., 2016. Aliphatics hydrocarbon content in surface sediment from Jakarta Bay, Indonesia, in: IOP Conference Series: Materials Science and Engineering. IOP Publishing, p. 12007.

Zaghloul, Z.M., Shaaban, F., Yossef, A., 2001. Mesozoic and Cenozoic sedimentary basins of the Nile Delta, Egypt, in: Deltas Modem and Ancient. Proc. Mansoura Univ. 1st Internat. Symp. on Deltas, Cairo, Egypt. pp. 21–33.

Zakaria, A., Ela, N.A., Mohamed, S.A., 2019. Biostratigraphy and sequence stratigraphy of the Oligocene succession, offshore Nile Delta, southeastern Mediterranean, Egypt, and its paleoenvironmental implications. Am. Assoc. Pet. Geol. Bull. 103, 2597–2625. https://doi.org/10.1306/02251918113

Zhao, Z., Grohmann, S., Zieger, L., Dai, W., Littke, R., 2022. Evolution of organic matter quantity and quality in a warm, hypersaline, alkaline lake: The example of the Miocene Nördlinger Ries impact crater, Germany. Front. Earth Sci. 10. https://doi.org/doi: 10.3389/feart.2022.989478

Zhao, Z., Littke, R., Zieger, L., Hou, D., Froidl, F., 2020. Depositional environment, thermal maturity and shale oil potential of the Cretaceous Qingshankou Formation in the eastern Changling Sag, Songliao Basin, China: An integrated organic and inorganic geochemistry approach. Int. J. Coal Geol. 232, 103621.